Electronic Supplementary Material (ESI) for Dalton Transactions.
This journal is © The Royal Society of Chemistry 2017

Electronic Supplementary Information (ESI) for:

Stable Au^{III} complexes with four *N*-heterocyclic carbene groups can be prepared in high yield directly from $KAuCl_4$.

Ahmed H. Mageed,[a,b] Brian W. Skelton[a,c] and Murray V. Baker[a]

a) School of Molecular Sciences M310, The University of Western Australia, 35 Stirling Highway, Perth, WA 6009, Australia.

b) Department of Chemistry, Faculty of Science, The University of Kufa, P.O. Box 21, Najaf 54001, Iraq.

c) Centre for Microscopy, Characterisation and Analysis M310, The University of Western Australia, Perth, WA 6009, Australia.

Table of Contents

	Page
NMR Spectra of complexes (Figures S1 - S12)	S2
Effect of chloride on ^{1}H NMR spectra of $[Au(\mathbf{L^1})_2Cl_2]Cl$ **2** in D_2O (Figure S13)	S14
H/D Exchange reactions of $[Au(\mathbf{L^1})_2Cl_2]Cl$ **2** (Figures S14 - S16)	S15
Stability studies (Figures S17-S23)	S18
Metal - Ligand Bond Lengths in some Distorted Octahedral Gold(III) Complexes. (Table S1)	S25
Cyclovoltammetric Studies (Figure S24)	S26
References	S28

NMR Spectra of complexes

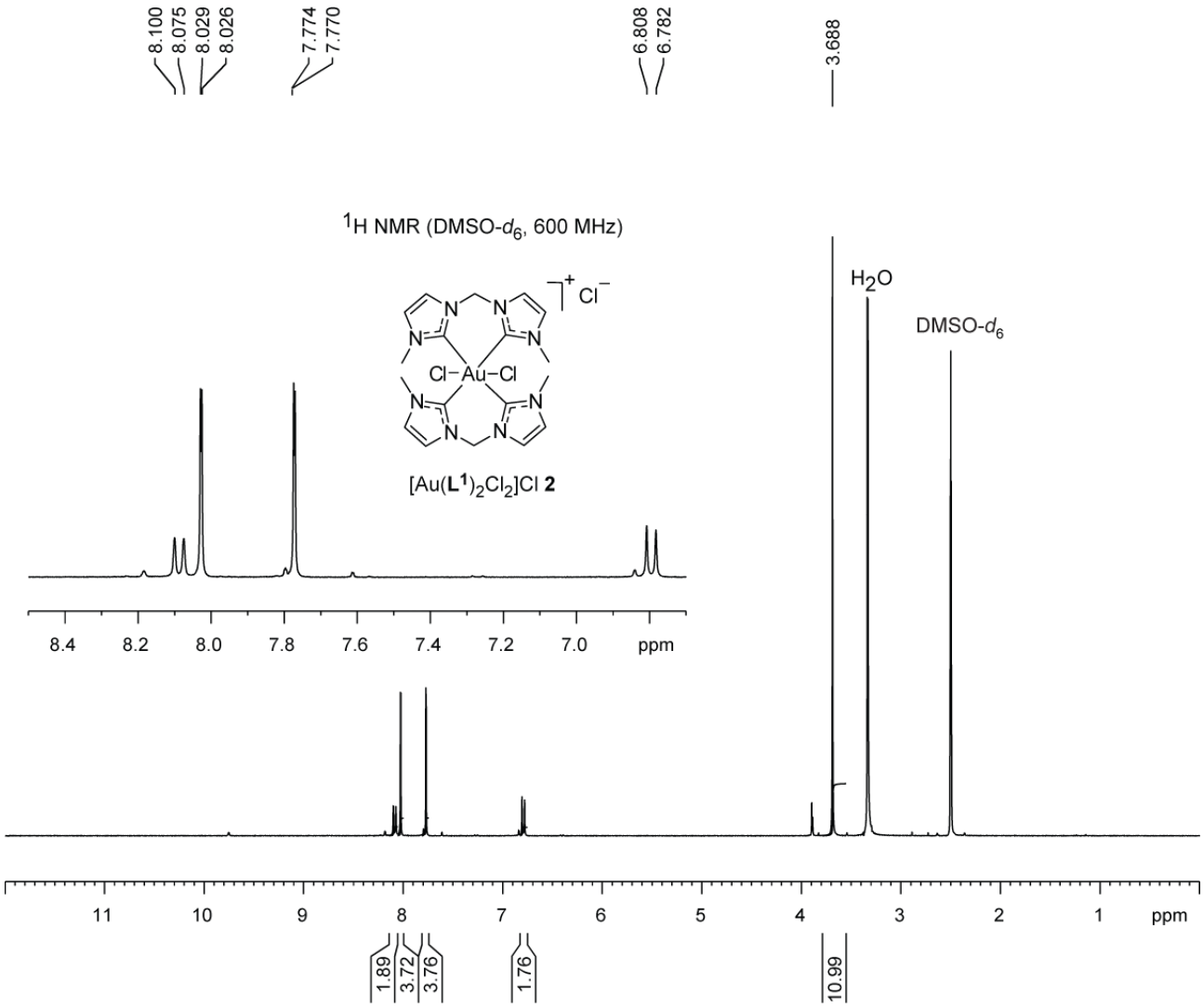

Figure S1. ^{1}H NMR spectrum of [Au(**L**^{1})$_2$Cl$_2$]Cl **2** in DMSO-d_6 at 600.13 MHz.

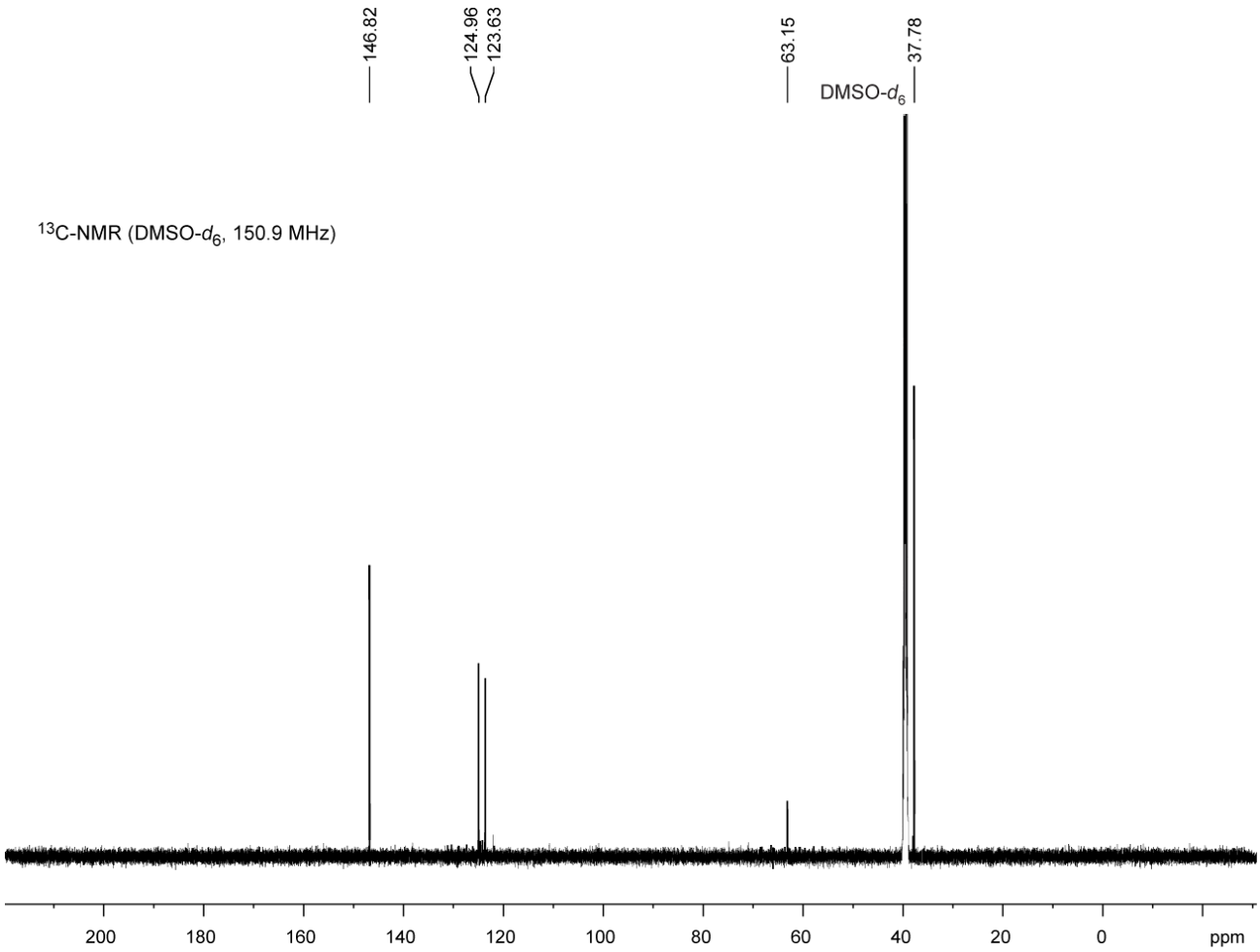

Figure S2. ^{13}C NMR spectrum of [Au(**L**^{1})$_2$Cl$_2$]Cl **2** in DMSO-d_6 at 125.77 MHz.

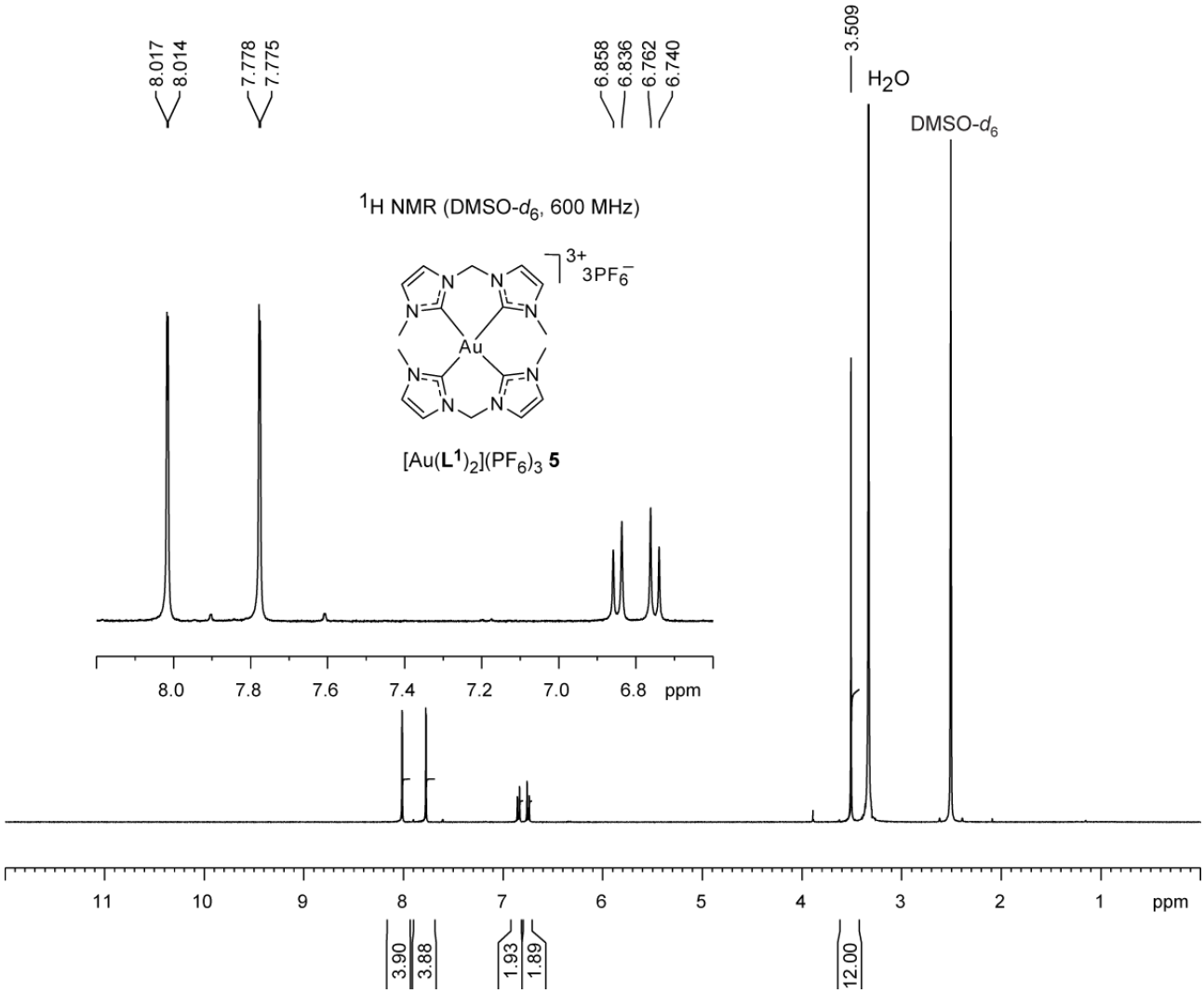

Figure S3. ^{1}H NMR spectrum of $[Au(\mathbf{L^1})_2](PF_6)_3$ **5** in DMSO-d_6 at 600.13 MHz.

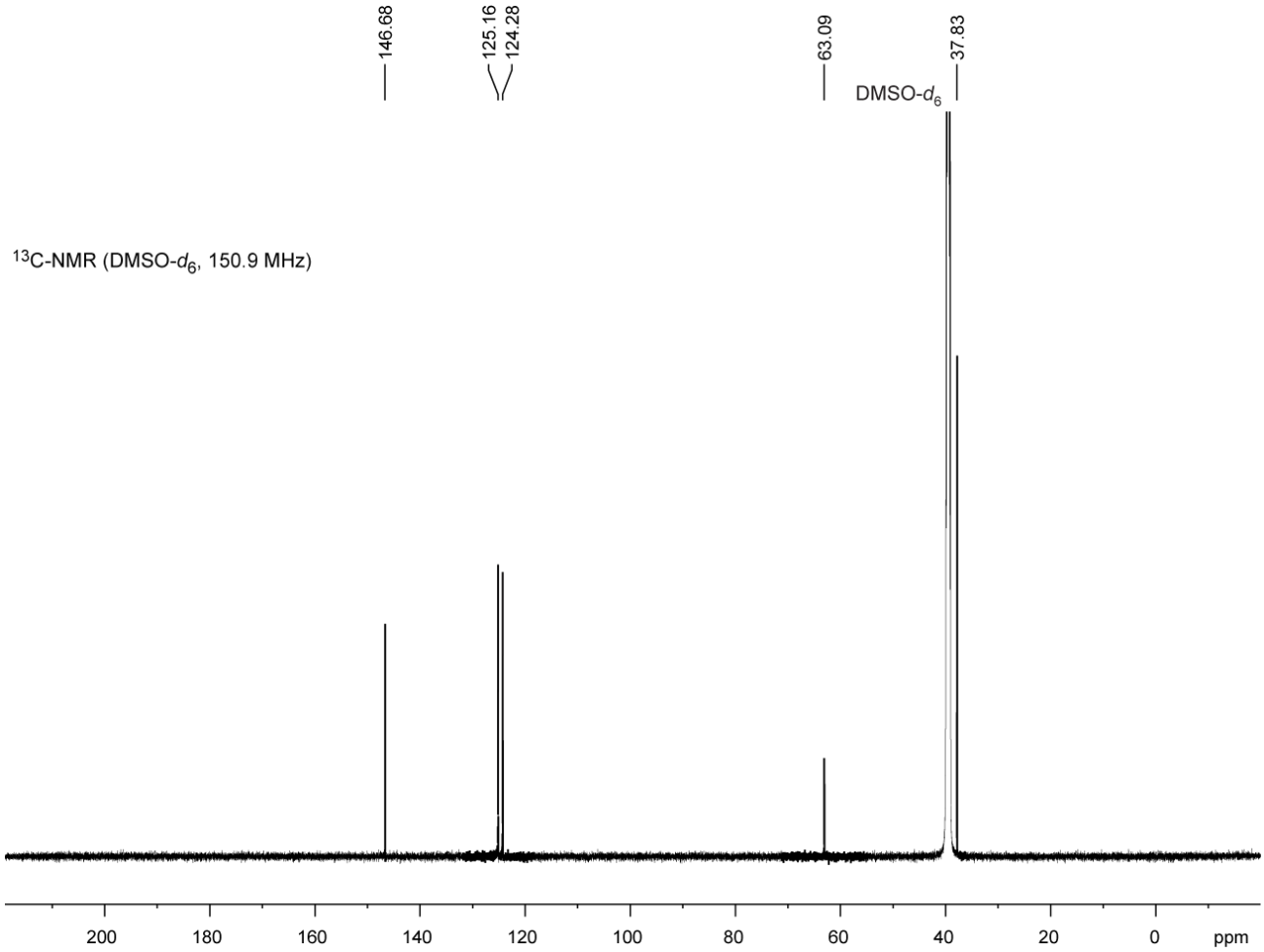

Figure S4. ^{13}C NMR spectrum of $[Au(\mathbf{L^1})_2](PF_6)_3$ **5** in DMSO-d_6 at 150.90 MHz.

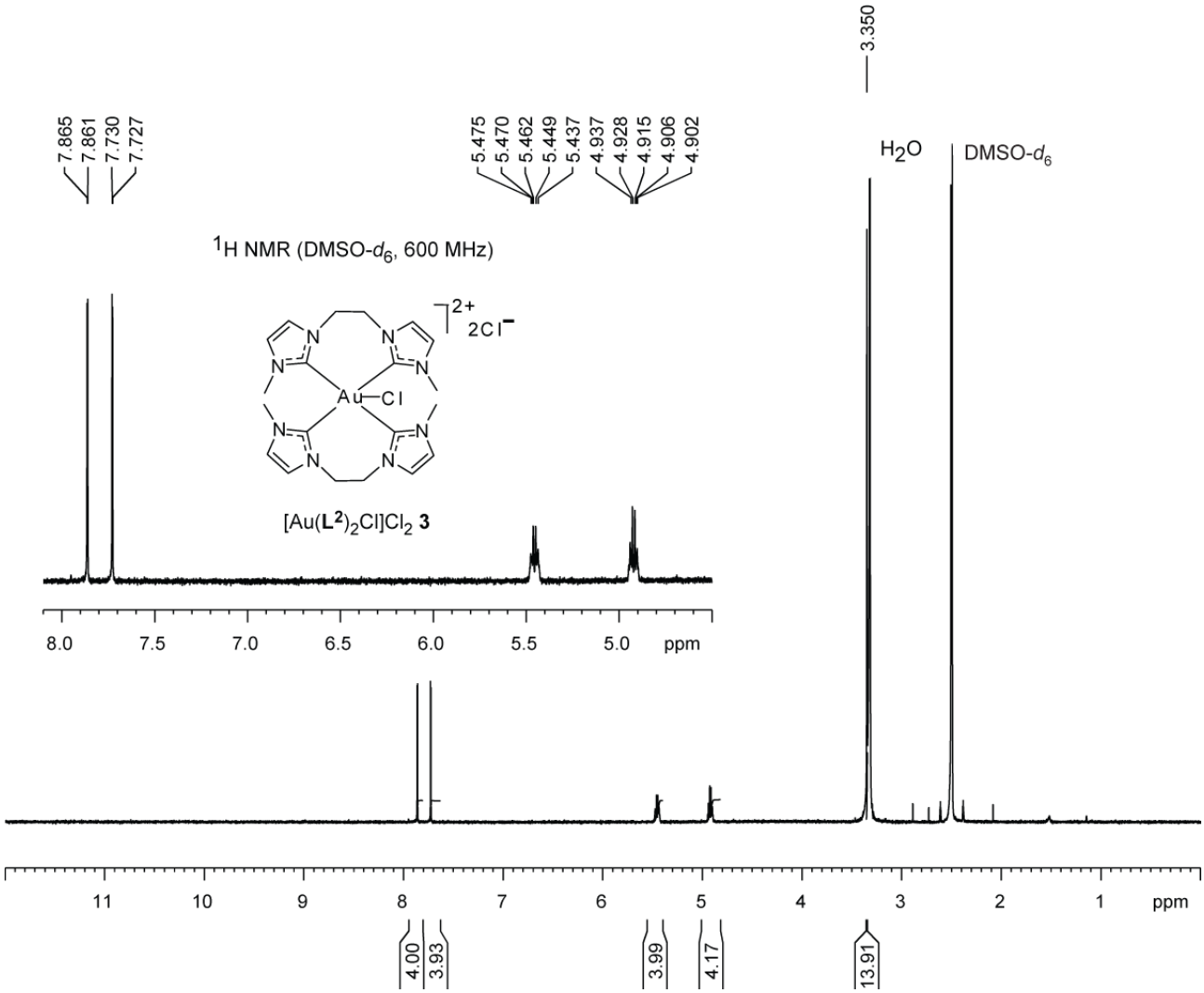

Figure S5. ^{1}H NMR spectrum of [Au(**L**^{2})$_2$Cl]Cl$_2$ **3** in DMSO-d_6 at 600.13 MHz.

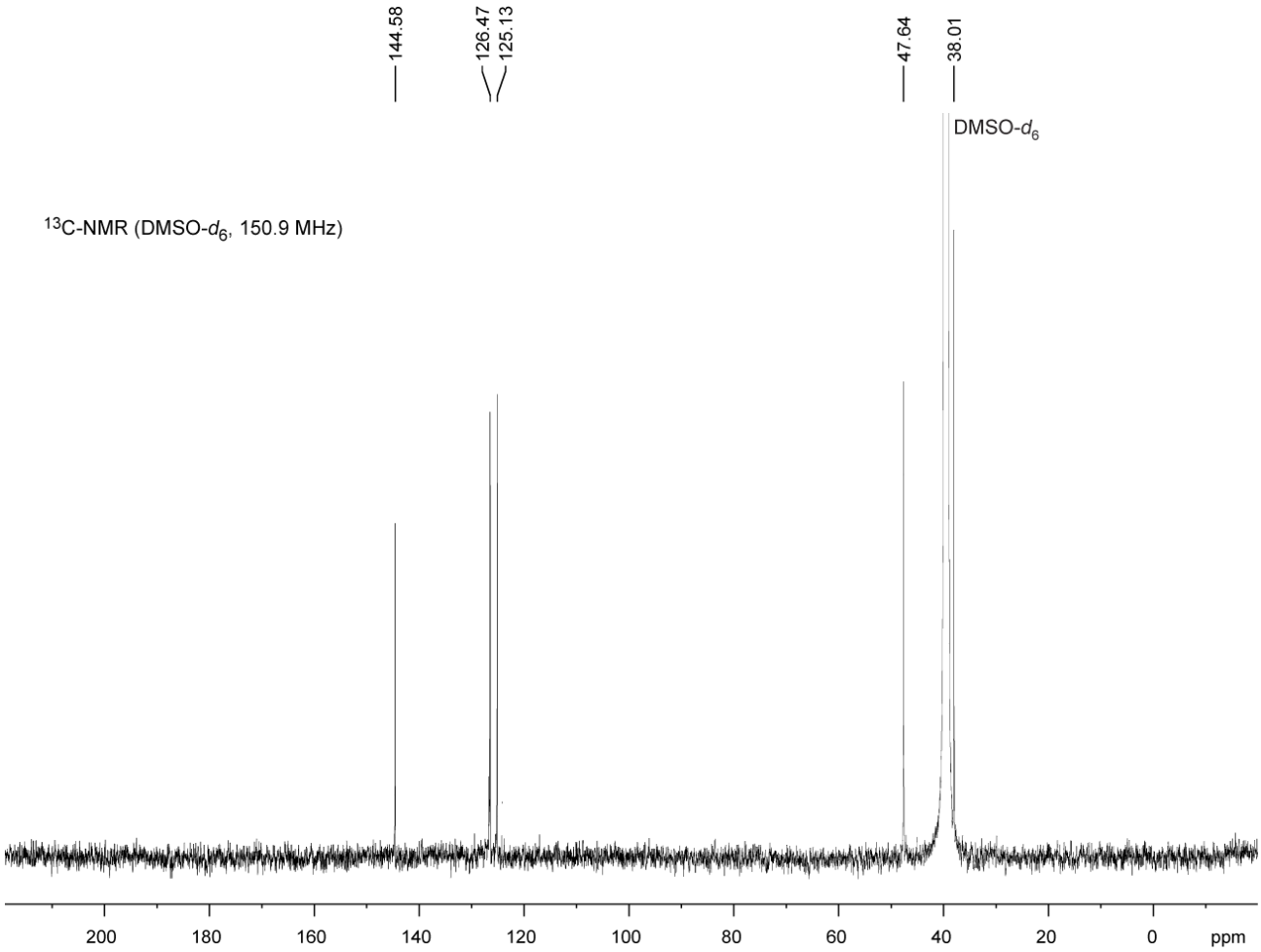

Figure S6. ^{13}C NMR spectrum of $[Au(\mathbf{L^2})_2Cl]Cl_2$ **3** in DMSO-d_6 at 150.90 MHz.

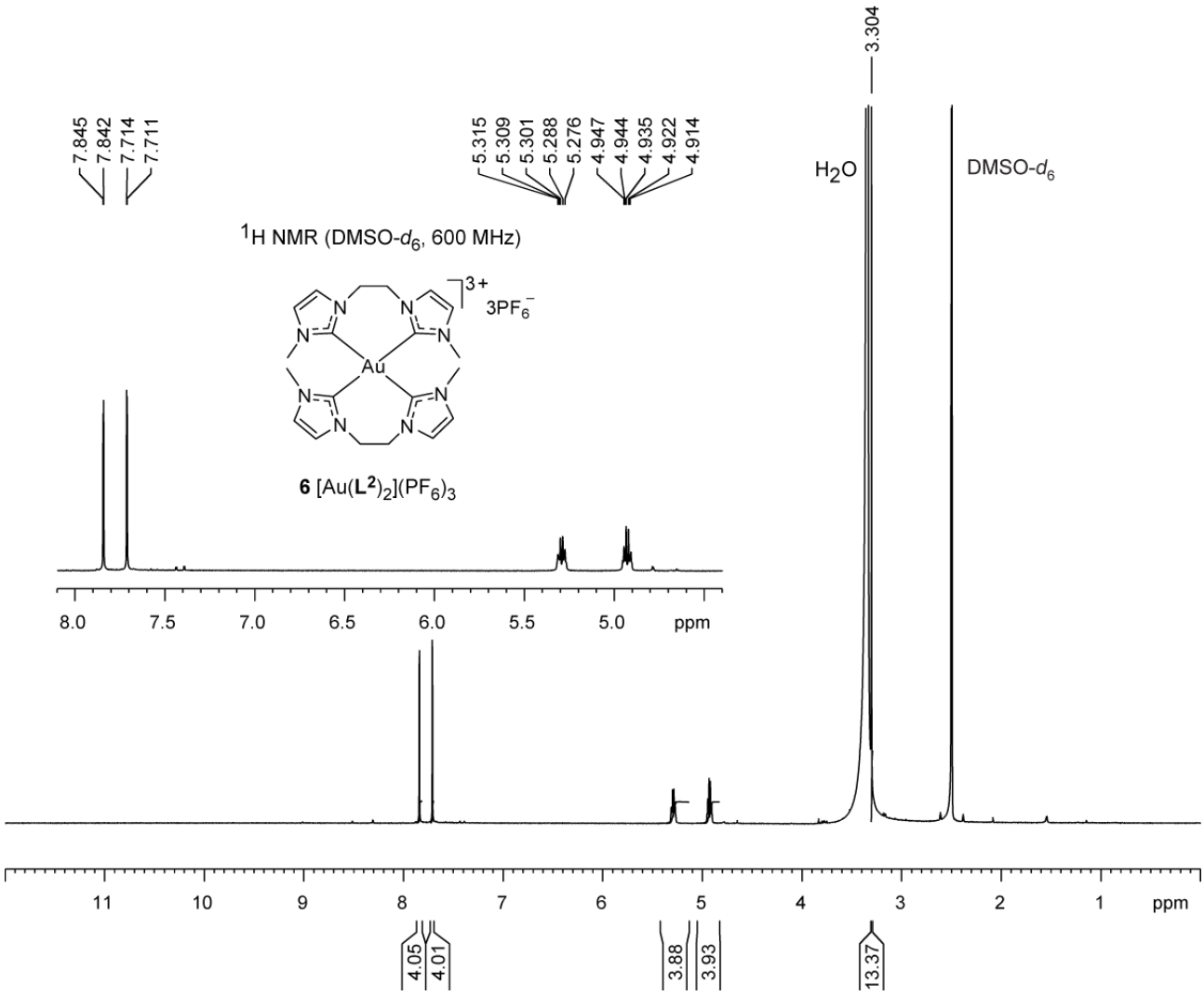

Figure S7. ^{1}H NMR spectrum of [Au(**L**^{2})$_2$](PF$_6$)$_3$ **6** in DMSO-d_6 at 600.13 MHz.

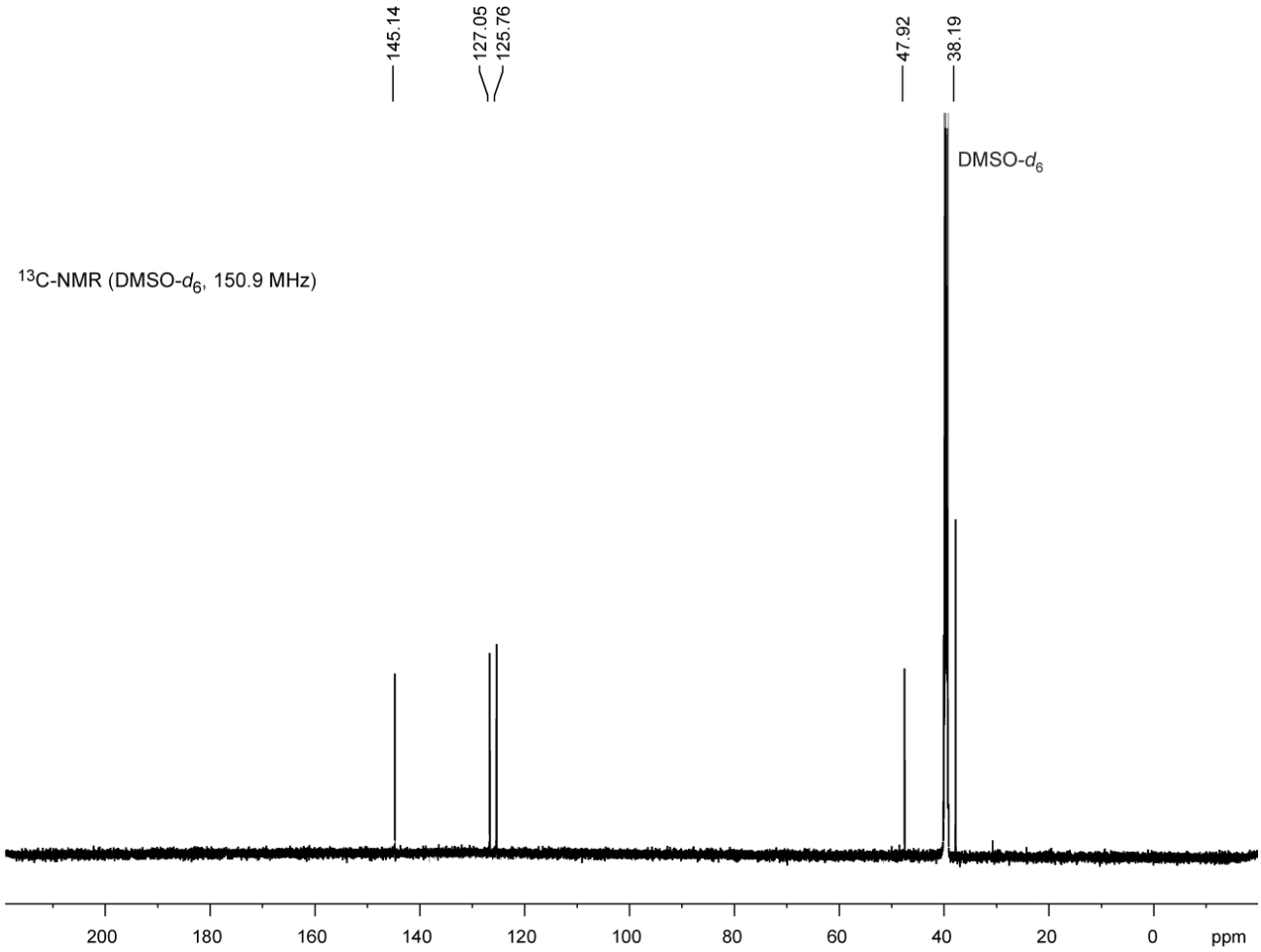

Figure S8. ^{13}C NMR spectrum of $[Au(\mathbf{L^2})_2](PF_6)_3$ **6** in DMSO-d_6 at 150.90 MHz.

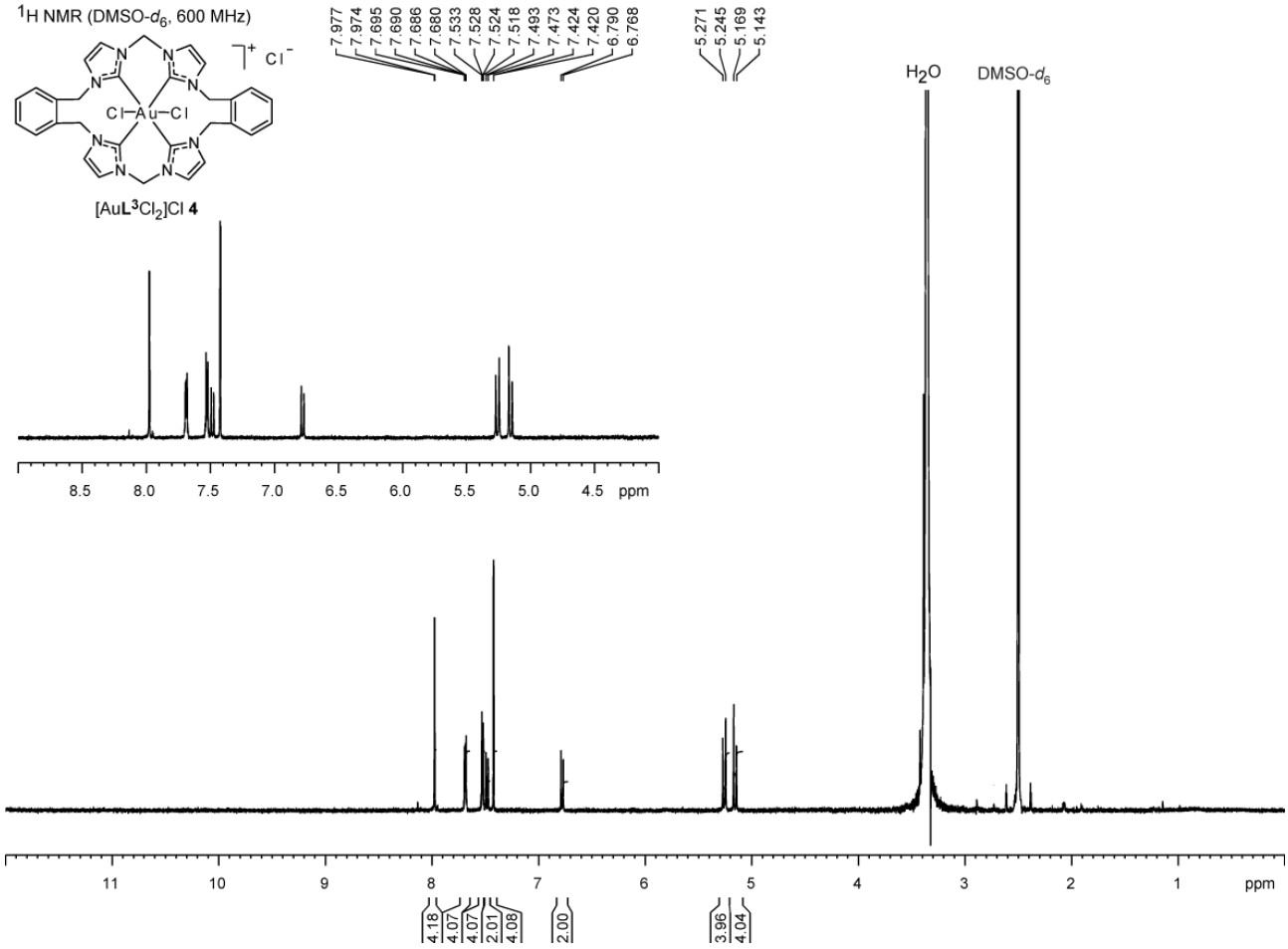

Figure S9. ^{1}H NMR spectrum of [Au**L**^{3}Cl$_2$]Cl **4** in DMSO-d_6 at 600.13 MHz.

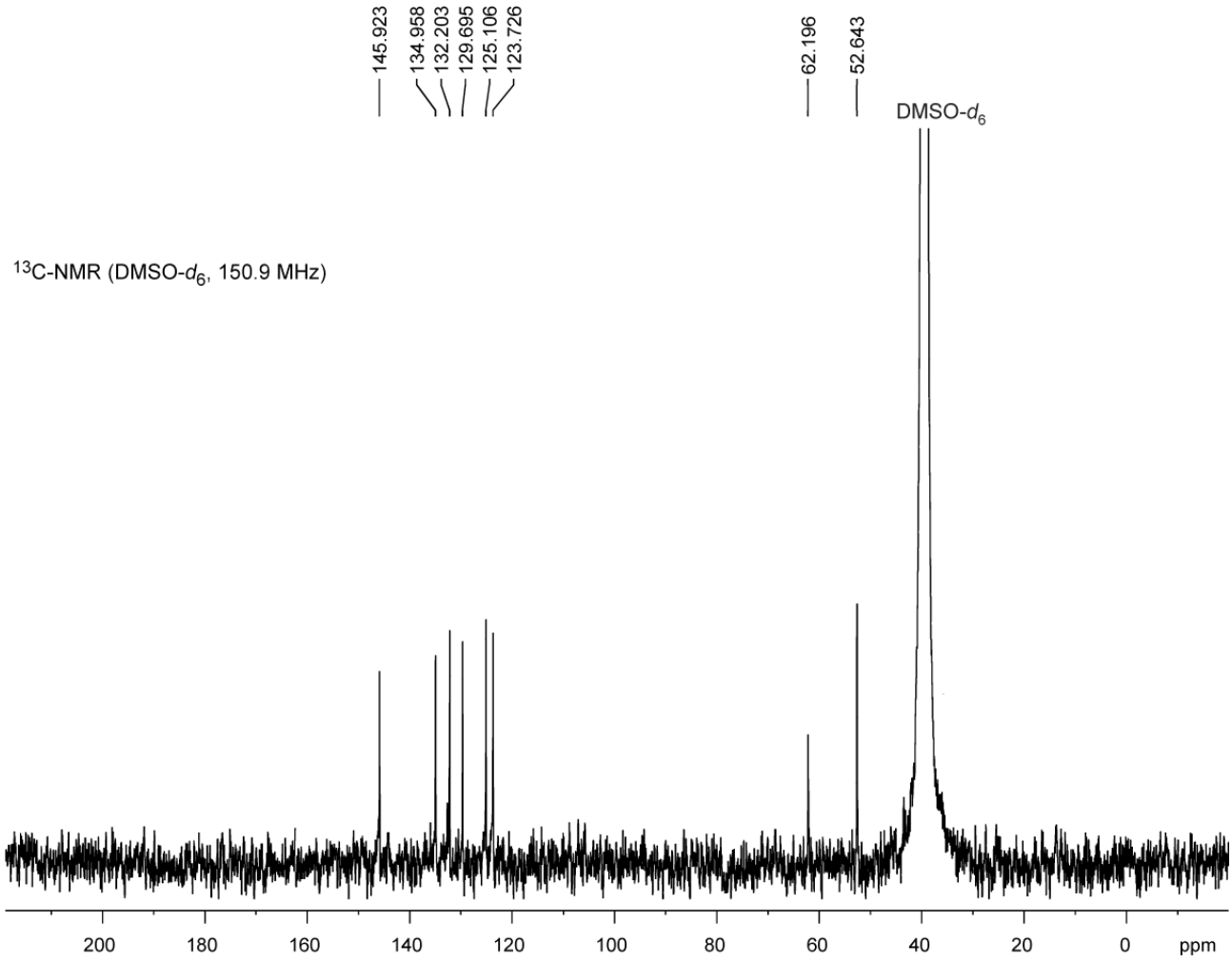

Figure S10. ^{13}C NMR spectrum of [Au**L**^{3}Cl$_2$]Cl **4** in DMSO-d_6 at 150.90 MHz.

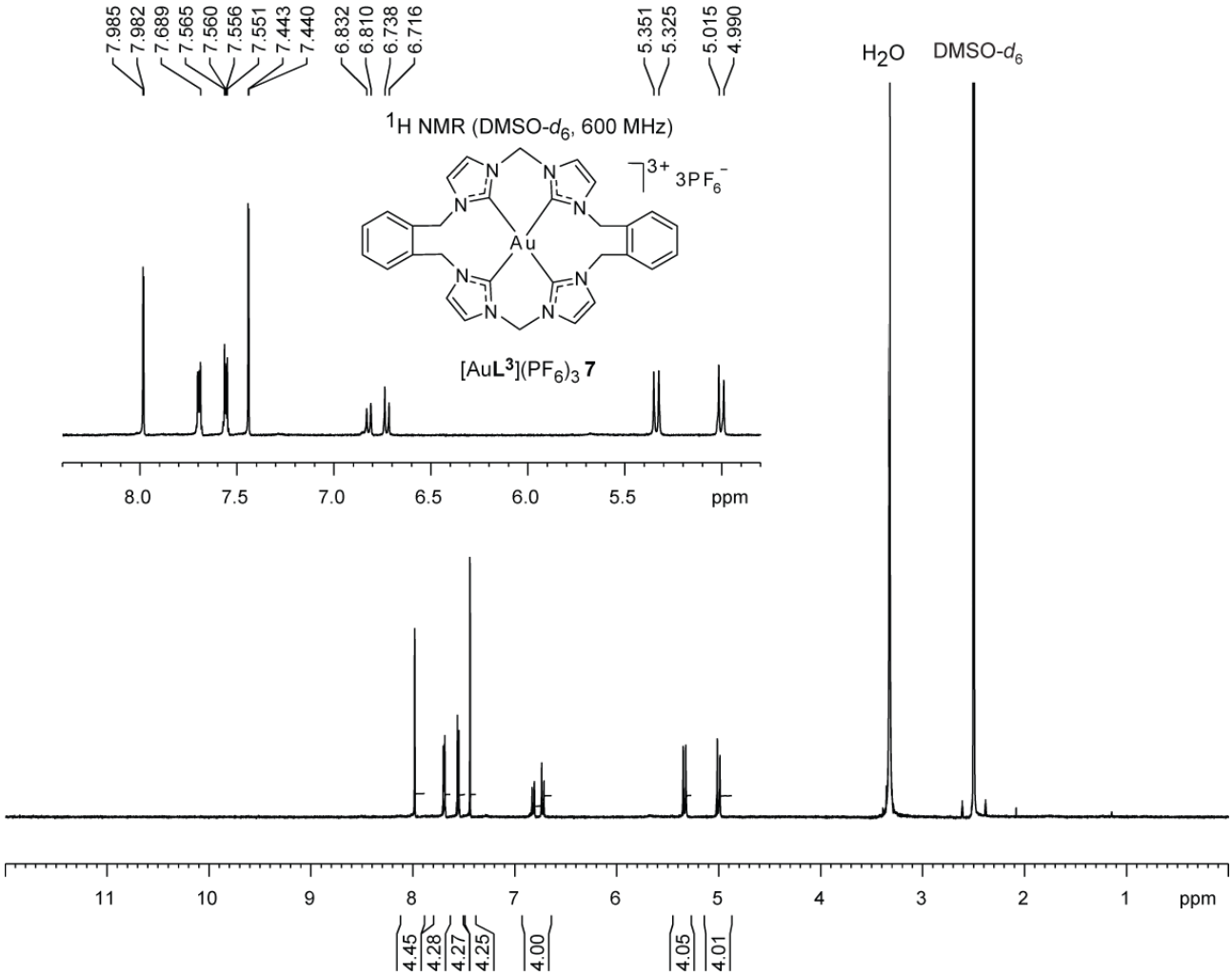

Figure S11. ^{1}H NMR spectrum of [Au**L**^{3}](PF$_6$)$_3$ **7** in DMSO-d_6 at 600.13 MHz.

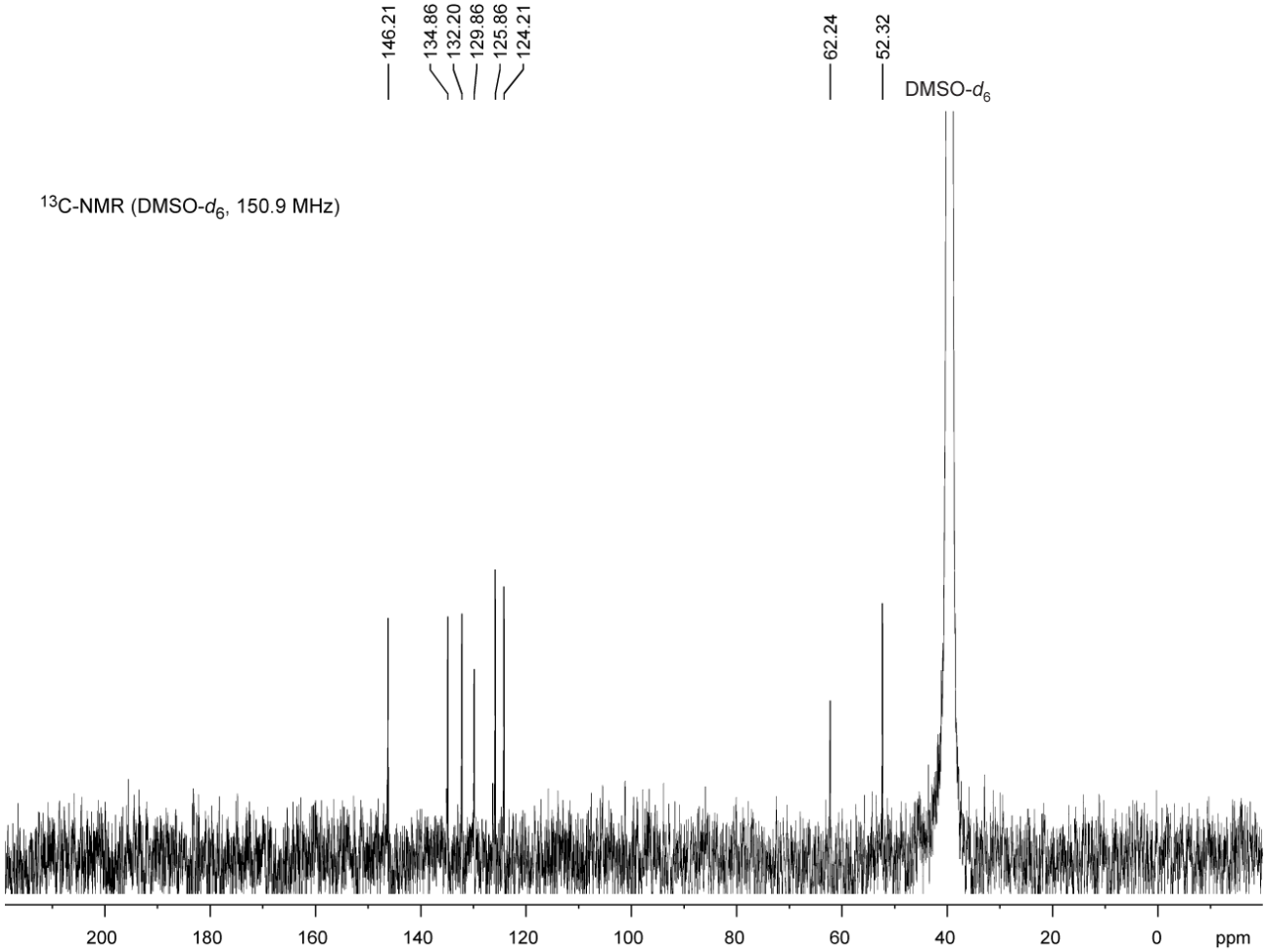

Figure S12. ^{13}C NMR spectrum of Au**L**^{3}](PF$_6$)$_3$ **7** in DMSO-d_6 at 150.90 MHz.

Effect of chloride on ^{1}H NMR spectra of $[Au(L^1)_2Cl_2]Cl$ 2 in D_2O

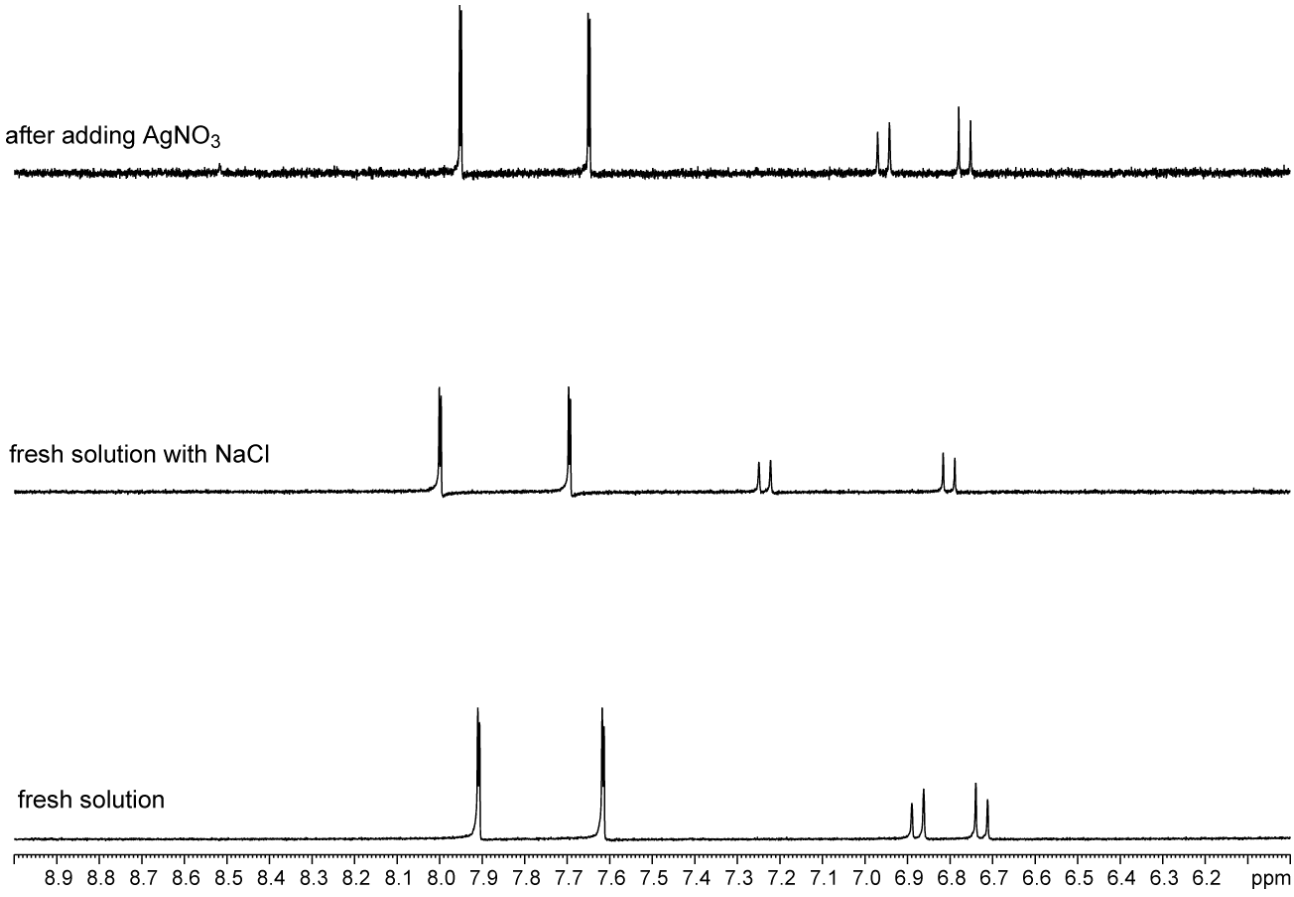

Figure S13. ^{1}H NMR spectra of $[Au(\mathbf{L^1})_2Cl_2]Cl$ **2** before and after adding NaCl and $AgNO_3$. Spectra were recorded using solutions of $[Au\mathbf{L^1}Cl_2]Cl$ **2** in D_2O at 600.13 MHz.

H/D Exchange reactions of $[Au(L^1)_2Cl_2]Cl$ 2

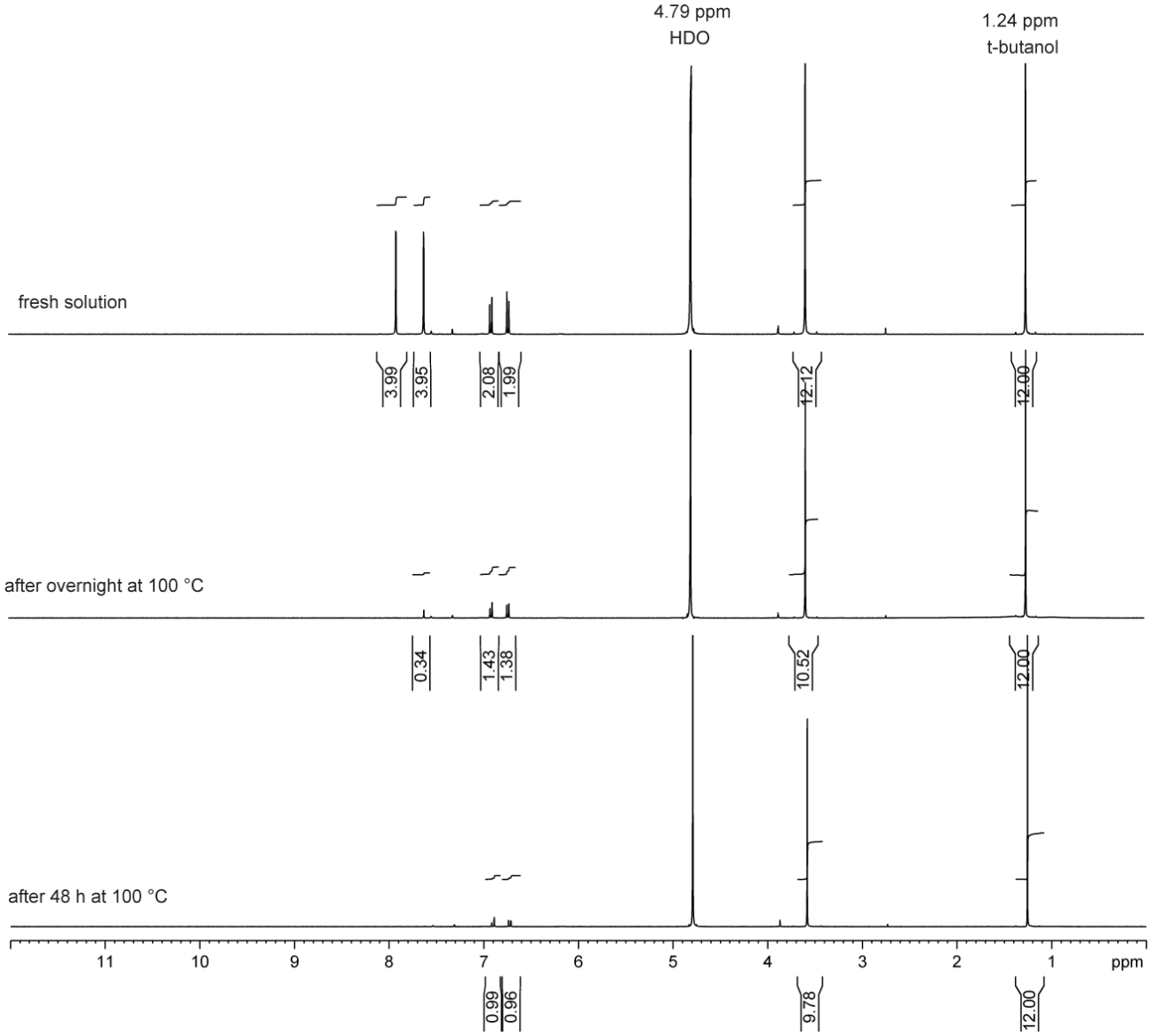

Figure S14. ^1H NMR spectra of $[Au(\mathbf{L^1})_2Cl_2]Cl$ **2** before and after H/D exchange. Spectra were recorded using solutions of complex $[Au(\mathbf{L^1})_2Cl_2]Cl$ **2** in D_2O at 600.13 MHz and internal standard (t-butanol) at ambient temperature. Conditions required for complete exchange of the protons: CH_2 = D_2O, 100 °C, 48 h ; H4/H5 = D_2O, 100 °C, 17 h.

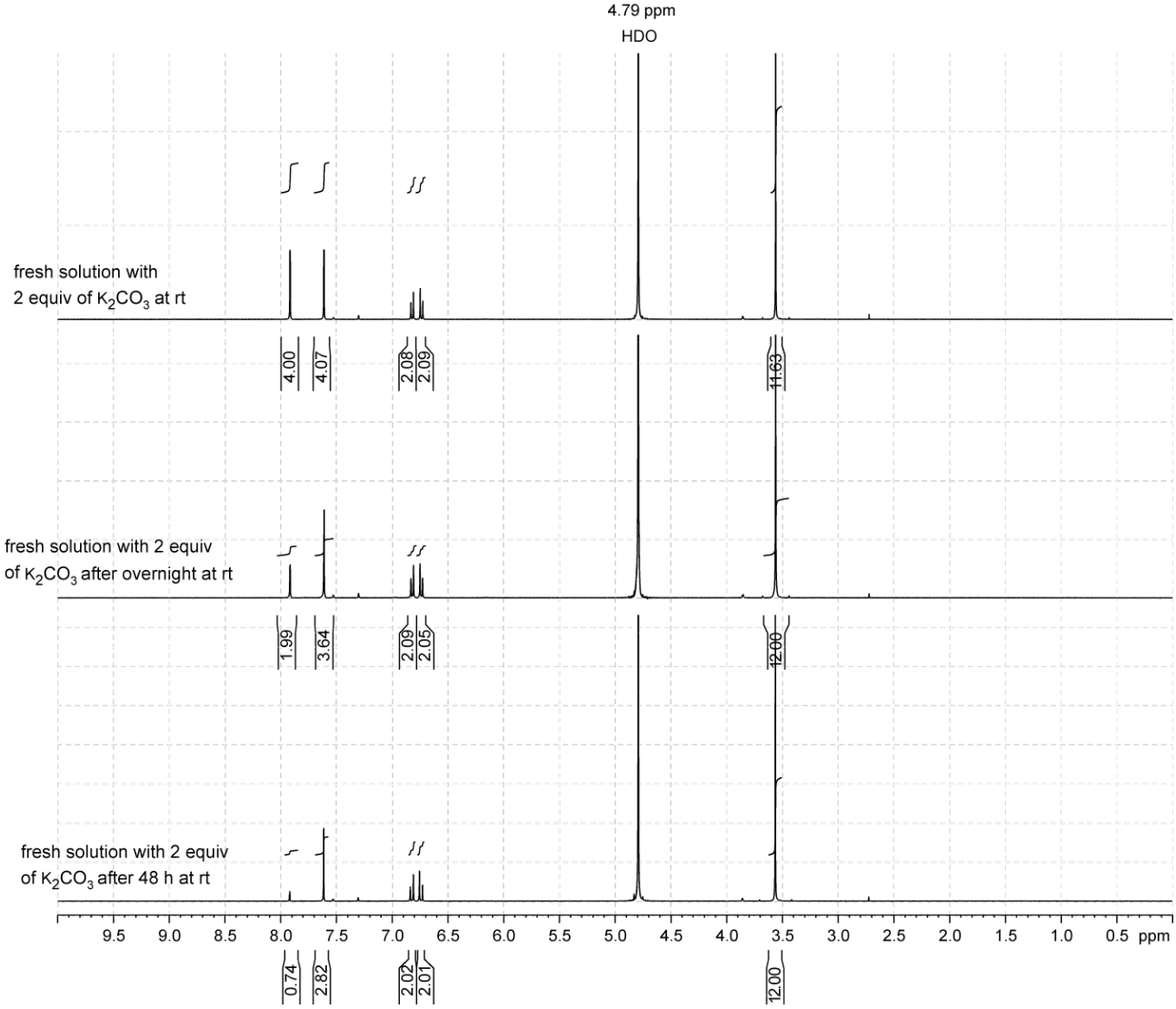

Figure S15. ^{1}H NMR spectra of [Au(**L**^{1})$_2$Cl$_2$]Cl **2** before and after H/D exchange. Spectra were recorded using solutions of [Au(**L**^{1})$_2$Cl$_2$]Cl **2** in D_2O at 600.13 MHz and ambient temperature. Conditions required for complete exchange of the protons: H4/H5 = D_2O, 2 equiv of K_2CO_3, room temperature, 48h.

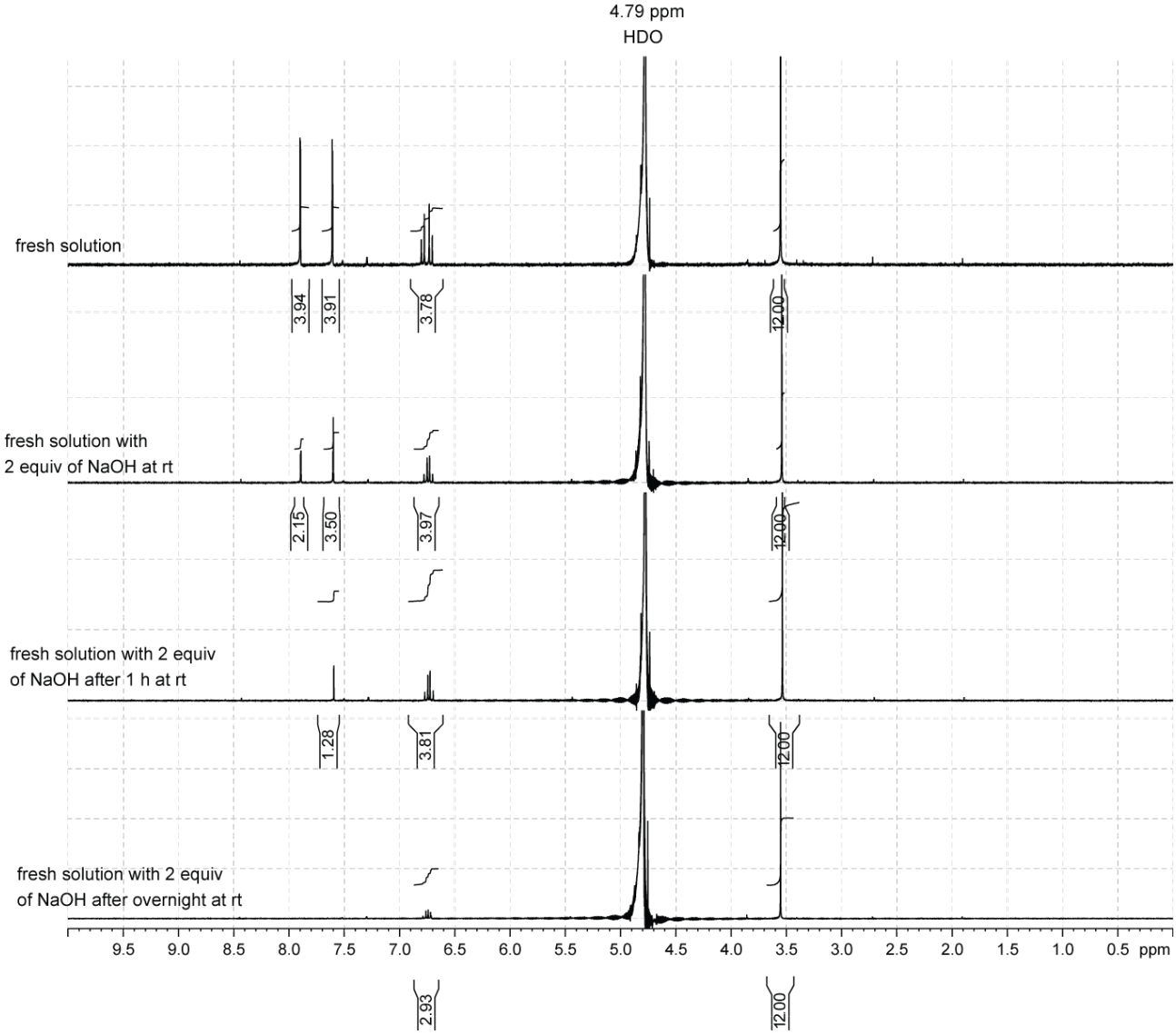

Figure S16. ^{1}H NMR spectra of [Au(**L**^{1})$_2$Cl$_2$]Cl **2** before and after H/D exchange. Spectra were recorded using solutions of [Au(**L**^{1})$_2$Cl$_2$]Cl **2** in D_2O at 600.13 MHz and ambient temperature. Conditions required for complete exchange of the protons: H4/H5 = D_2O, 2 equiv of NaOH, room temperature, overnight.

Stability studies

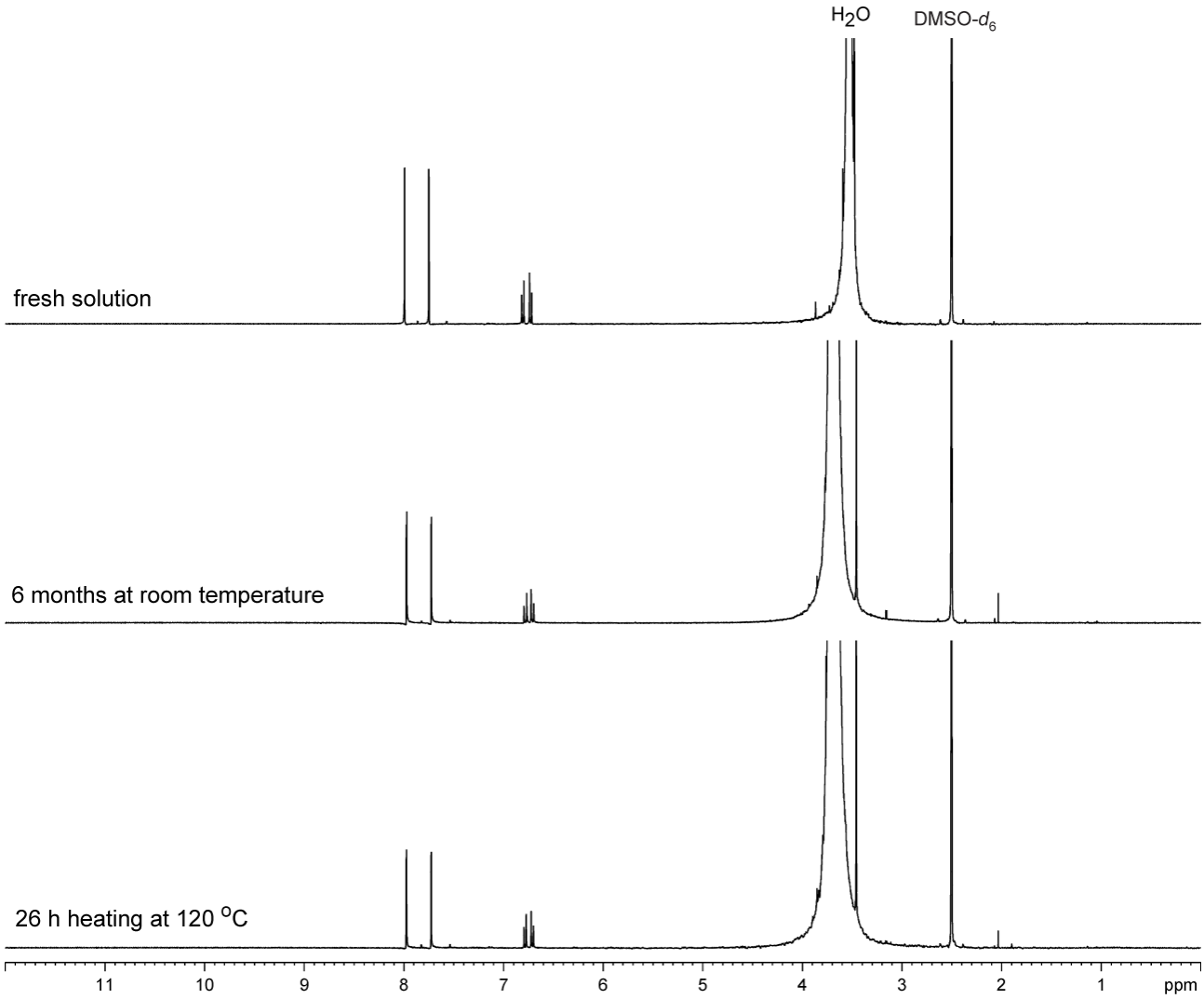

Figure S17. ^{1}H NMR spectra (DMSO-d_6, 600.13 MHz) of a sample of $[Au(\mathbf{L^1})_2](PF_6)_3$ **5**.

Top: Freshly prepared solution.

Middle: The same solution, after storage on the bench for 6 months at room temperature.

Bottom: The same solution, after being heated for 26 h at 120 °C.

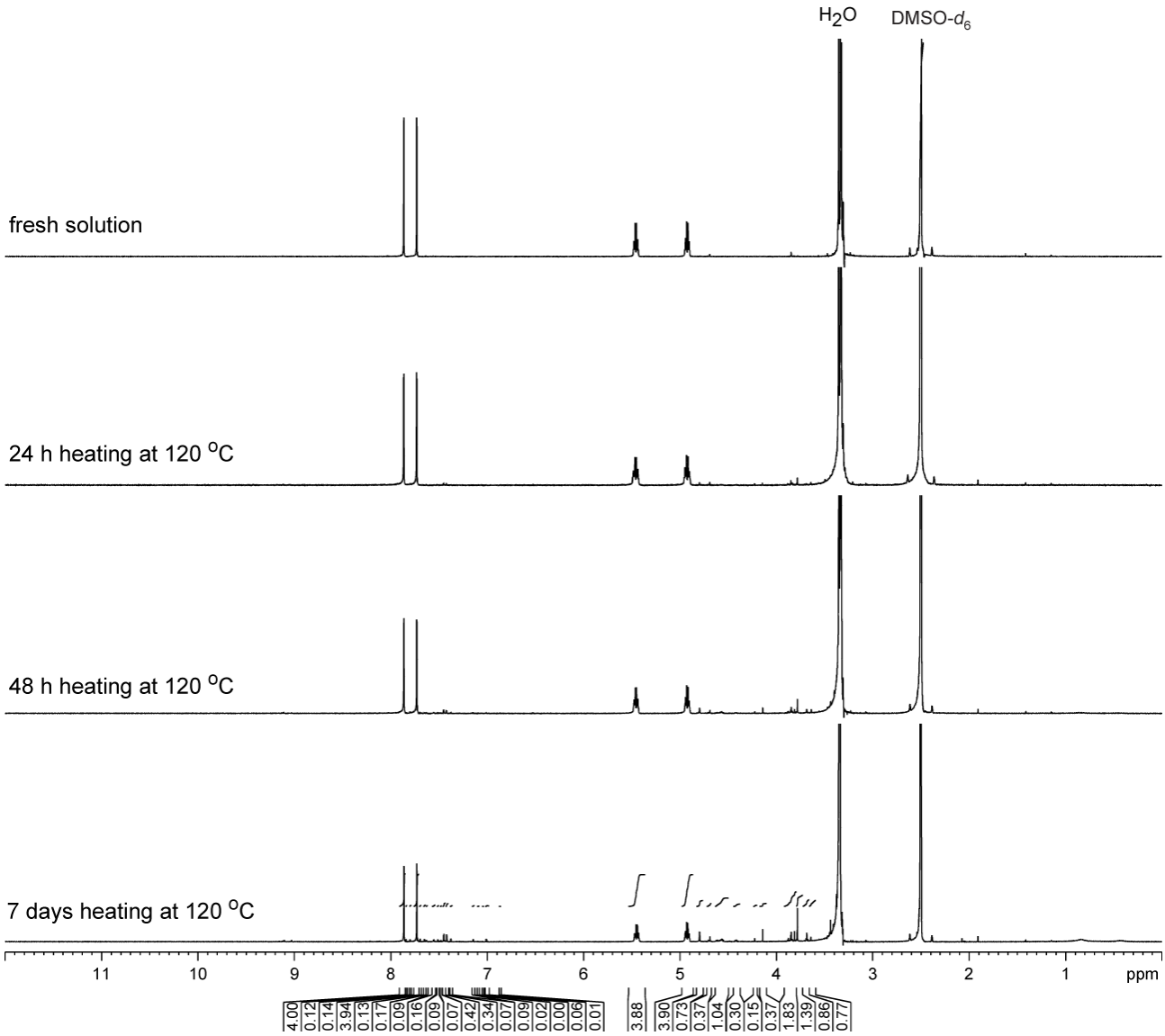

Figure S18. ^{1}H NMR spectra (DMSO-d_6, 600.13 MHz) of a sample of $[Au(\mathbf{L^2})_2Cl_2]Cl$ **3**.

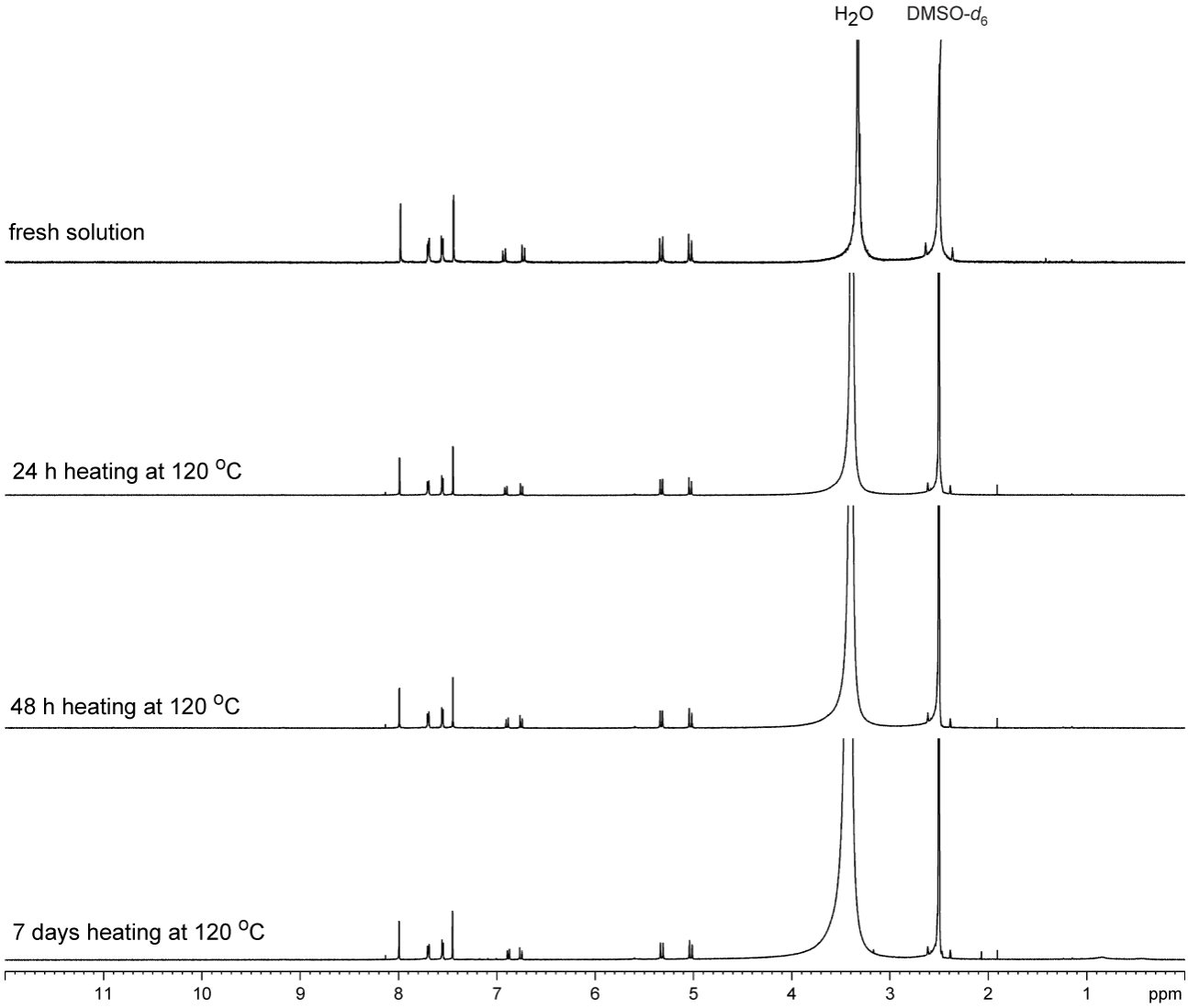

Figure S19. ^{1}H NMR spectra (DMSO-d_6, 600.13 MHz) of a sample of [Au(**L**^{3})](PF_6)$_3$ **7**.

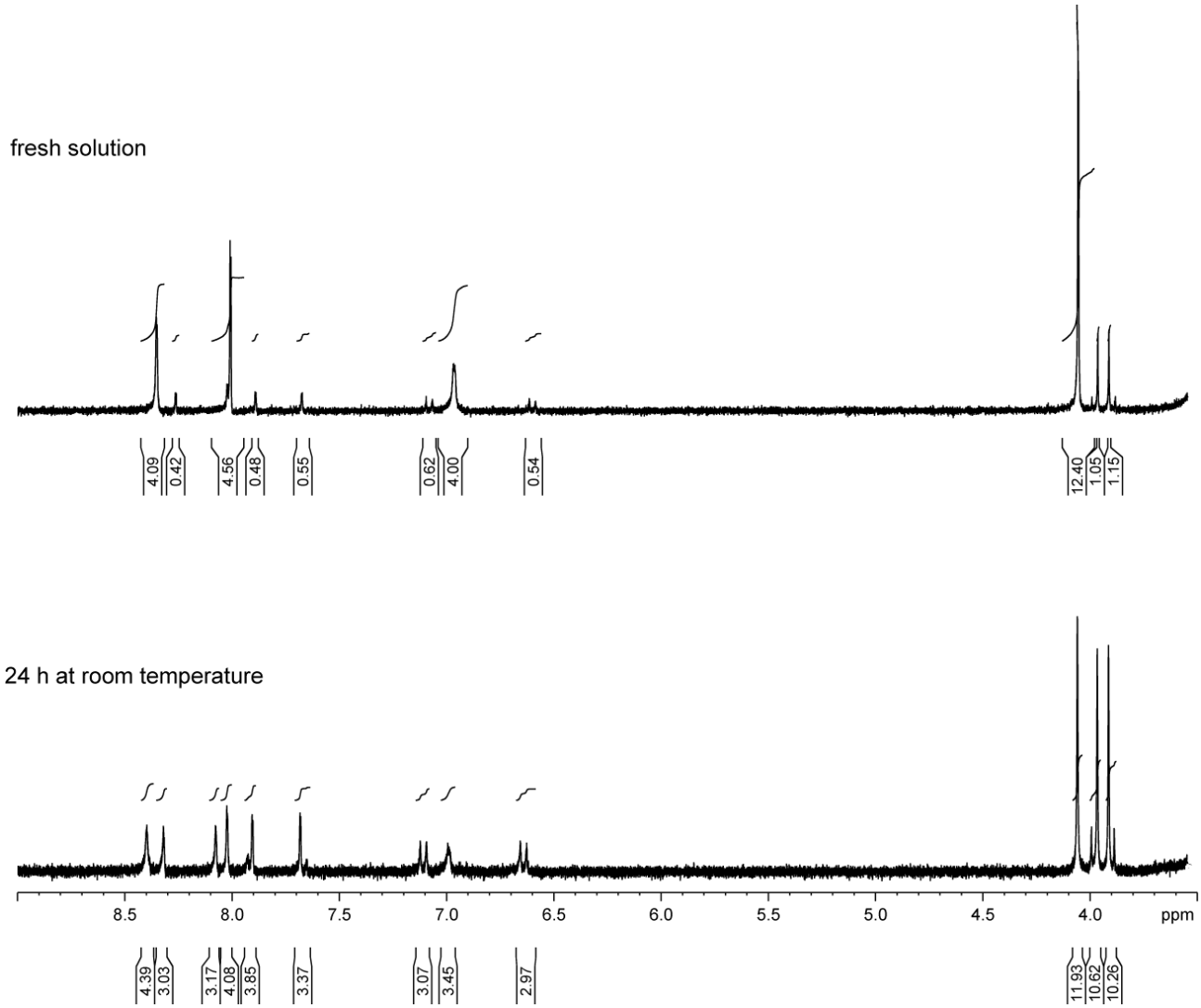

Figure S20. ^{1}H NMR spectra (DMSO-d_6, 600.13 MHz) of a sample of $[Au_2(\mathbf{L^1})_2Br_4]Br_2$.

Top: Fresh solution prepared from solid $[Au_2(\mathbf{L^1})_2Br_4]Br_2$. The solid had been stored at room temperature on the bench for 1 month, and had partly decomposed prior to the solution being prepared, so the spectrum shows signals due to the Au^{III}/Au^{III} complex $[Au_2(\mathbf{L}^1)_2Br_4]^{2+}$ (near 8.35, 8.00, 6.96, and 4.05 ppm) and minor signals due to its Au^{I}/Au^{III} decomposition product $[Au_2(\mathbf{L^1})_2Br_2]^{2+}$.

Bottom: The same solution, after storage on the bench for 24 h at room temperature.

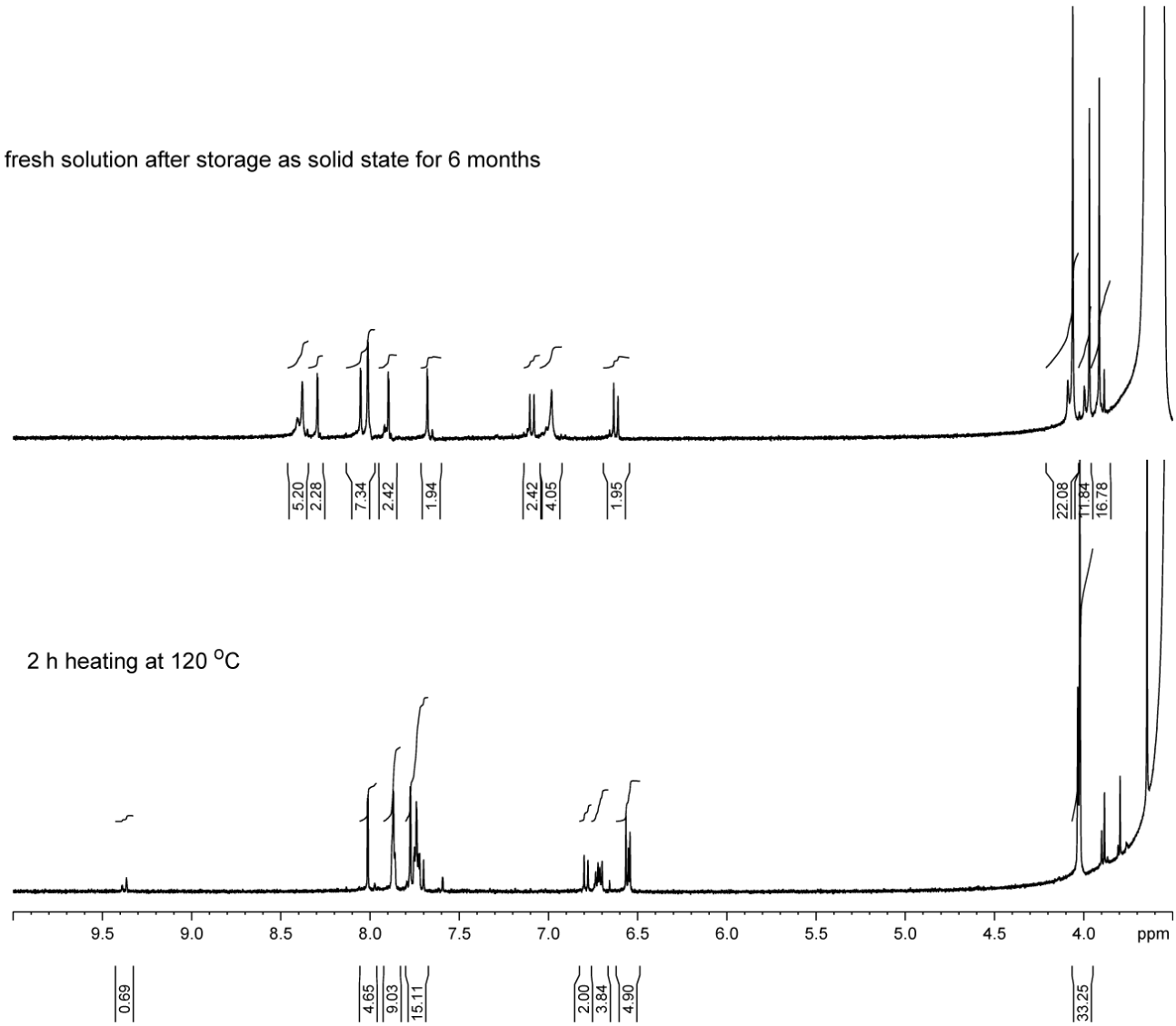

Figure S21. ^{1}H NMR spectra (DMSO-d_6, 600.13 MHz) of a sample of $[Au_2(\mathbf{L^1})_2Br_4]Br_2$.

Top: Fresh solution prepared from solid $[Au_2(\mathbf{L^1})_2Br_4]Br_2$ that had been stored in a sealed vial at room temperature on the bench for 6 months.

Bottom: The same solution, after heating for 2 h at 120 °C.

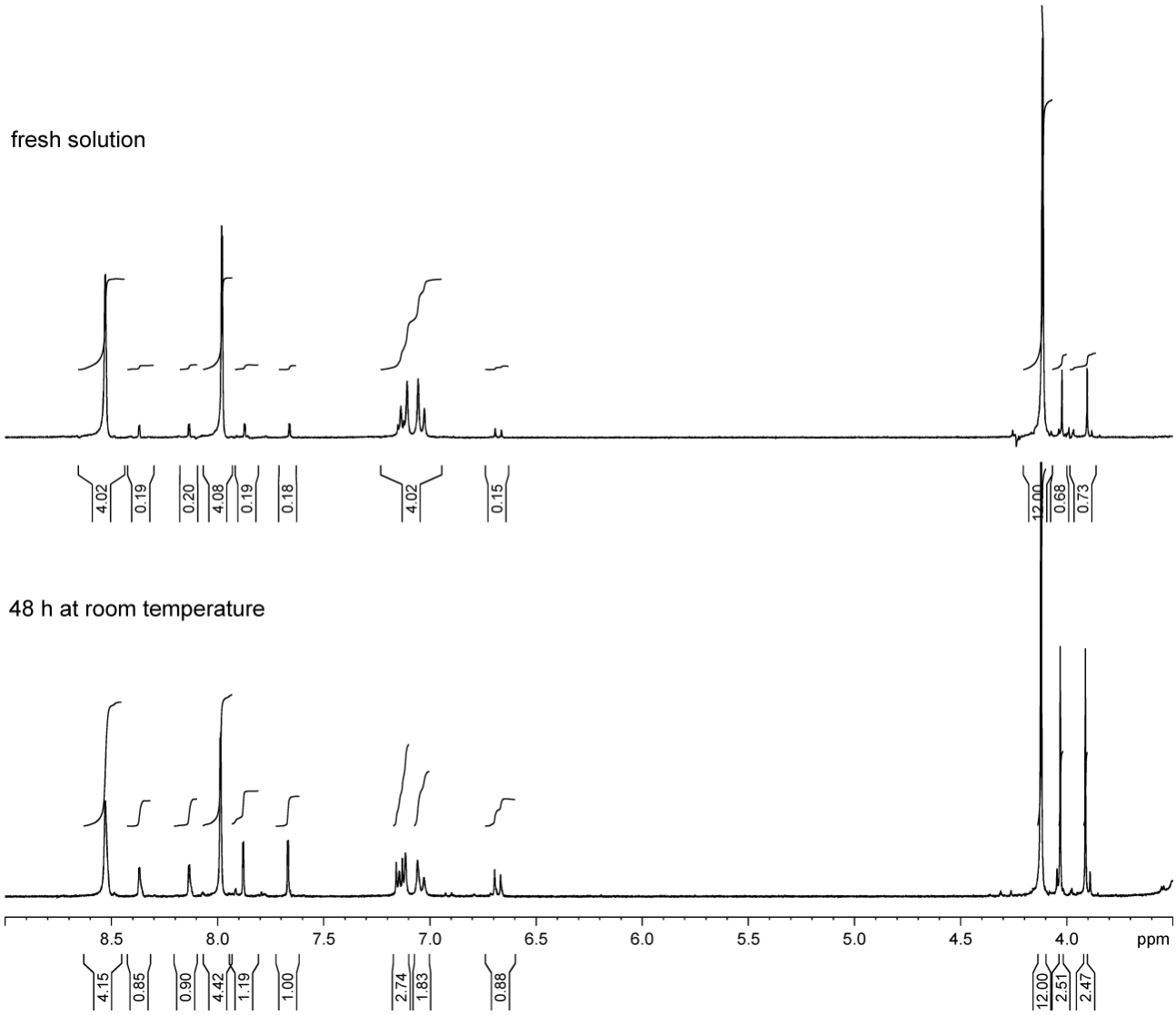

Figure S22. ^{1}H NMR spectra (DMSO-d_6, 600.13 MHz) of a sample of $[Au_2(\mathbf{L^1})_2Cl_4]Cl_2$.

Top: Fresh solution prepared from solid $[Au_2(\mathbf{L^1})_2Cl_4]Cl_2$ that had been stored in a sealed vial at room temperature on the bench for 1 month.

Bottom: The same solution, after 48 h at room temperature.

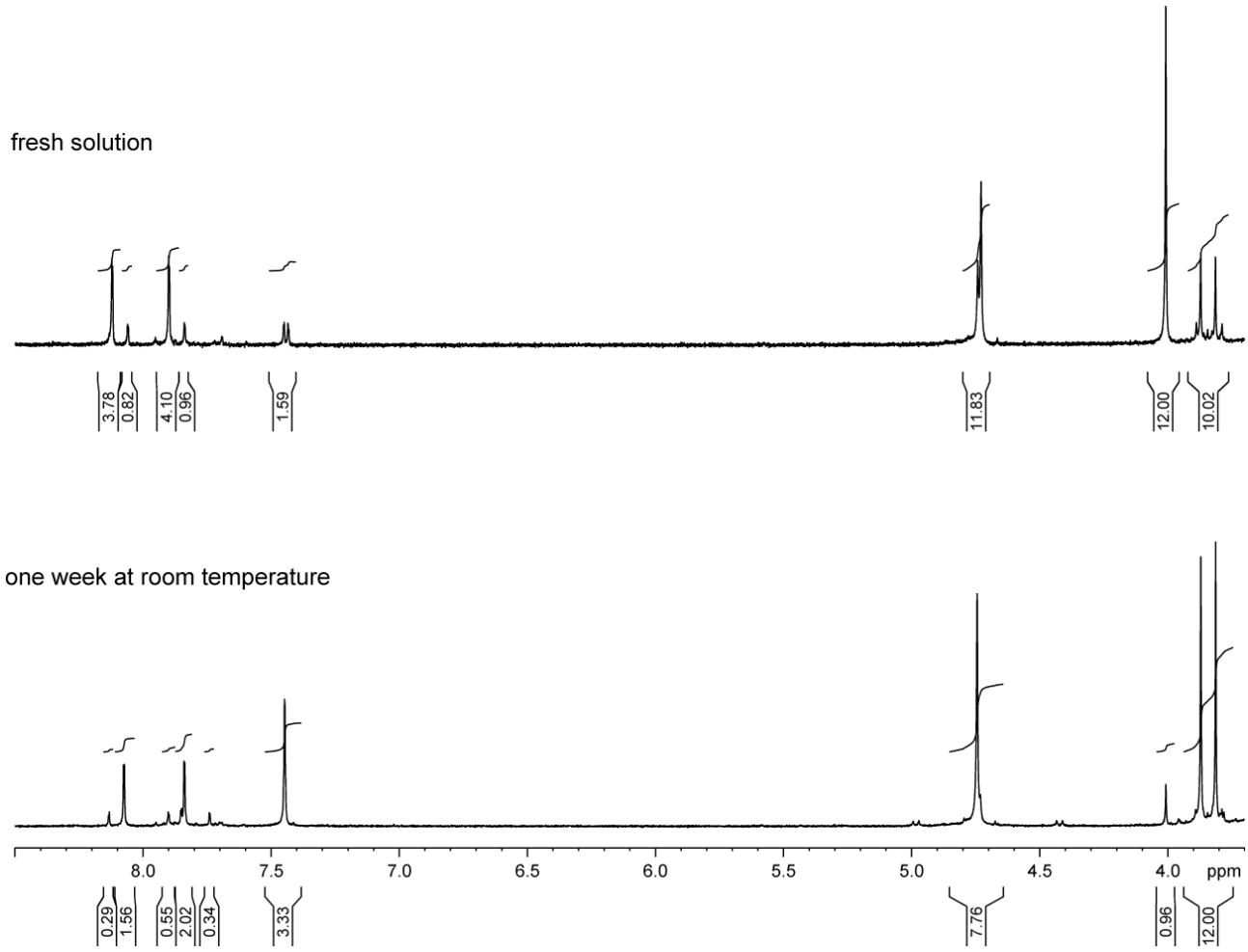

Figure S23. ^{1}H NMR spectra (DMSO-d_6, 600.13 MHz) of a sample of $[Au_2(\mathbf{L^2})_2Br_4]Br_2$.

Top: Fresh solution prepared from solid $[Au_2(\mathbf{L^2})_2Br_4]Br_2$ that had been stored in a sealed vial at room temperature on the bench for 1 week.

Bottom: The same solution, after storage for one week on the bench at room temperature.

Table S1. Metal - Ligand Bond Lengths (Å) in some Distorted Octahedral Gold(III) Complexes.

Complex [a]	Au-L_{axial}	Au-$L_{equatorial}$	Ref.
[Au(dien)C1$_3$]	3.183(3), 3.121(4) (Au-Cl)	2.278(3) (Au-Cl) 2.048(8), 2.010(8), 2.051(8) (Au-N)	1
[Au(dien)Cl_2(ClO_4)]	3.05 (Au-Cl) 3.10 (Au-$OClO_3$)	2.273(8) Au-Cl 1.97(2), 2.05(2), 1.98(2) (Au-N)	2
[Au(HHCT)Cl_2]$AuCl_4$	3.097(4) (Au-Cl)	2.043(11), 2.055(12) (Au-N)	3
trans-[Au(diars)$_2$$I_2$]I	3.35(2) (Au-I)	2.43(3), 2.46(2) (Au-As)	4

[a] Abbreviations: HHCT = 1,8-bis(hydroxyethyl)-1,3,6,8,10,13-hexaazacyclotetradecane; dien = diethylenetriamine; diars = 1,2-bis(dimethylarsinobenzene).

Cyclovoltammetric studies

Cyclic voltammetry experiments were recorded using an eDAQ e-corder 401 system in a three-electrode cell with a glassy carbon (1 mm diameter) working electrode, a platinum (1 mm diameter) counter electrode, and a platinum wire reference electrode. Measurements were taken at room temperature (25 °C) in acetonitrile with 0.1 M Bu_4NClO_4 as a supporting electrolyte.

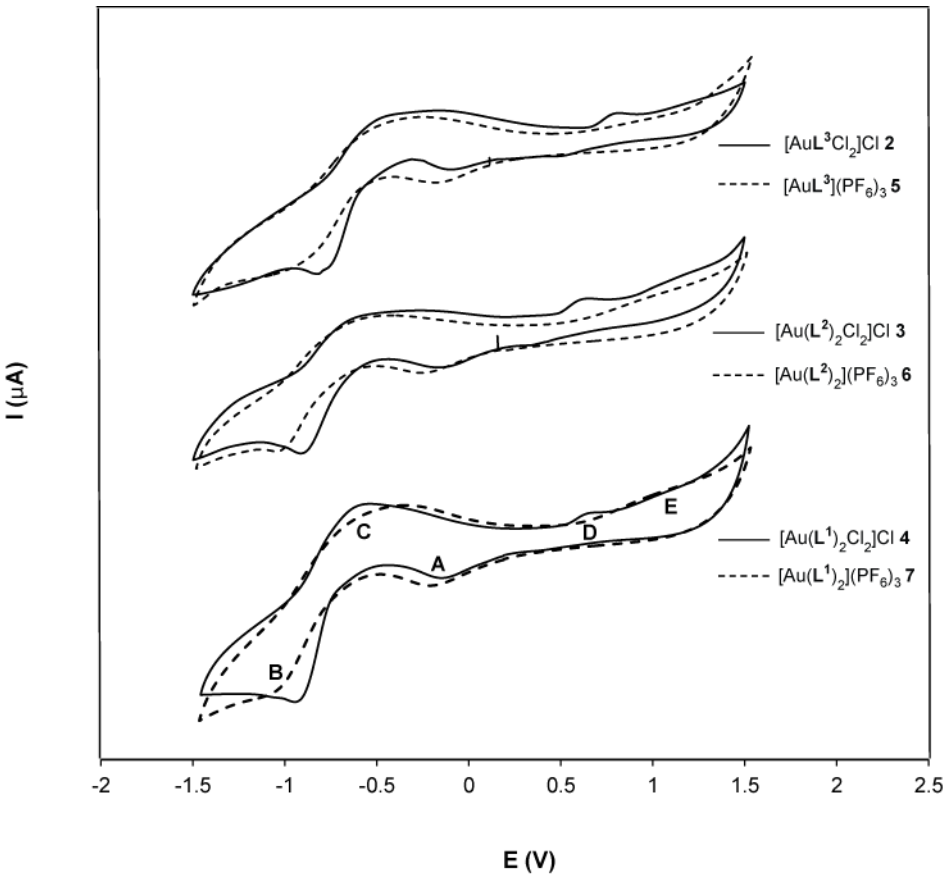

Figure S24. Overlaid cyclic voltammograms of Au^{III}-NHC complexes at 400 mV/s with 0.1 M nBu_4NClO_4 as a supporting electrolyte.

Table S2. Electrochemical properties of the Au^{III}-NHC complexes [a]

Complex	A	B	C	D	E
$[Au(\mathbf{L^1})_2Cl_2]Cl$ **2**	- 0.11	- 0.92	- 0.52	0.64	1.04
$[Au(\mathbf{L^1})_2](PF_6)_3$ **5**	- 0.22	- 1.03	- 0.41	-	0.99
$[Au(\mathbf{L^2})_2Cl_2]Cl$ **3**	- 0.10	- 0.89	- 0.55	0.66	1.14
$[Au(\mathbf{L^2})_2](PF_6)_3$ **6**	- 0.19	- 1.08	- 0.49	-	1.06
$[Au\mathbf{L^3}Cl_2]Cl$ **4**	- 0.09	- 0.78	- 0.56	0.71	1.12
$[Au\mathbf{L^3}](PF_6)_3$ **7**	- 0.21	- 0.89	- 0.43	-	1.09

[a] Measured in MeCN at a scan rate of 400 mV/s with 0.1 M nBu$_4$NClO$_4$, as a supporting electrolyte.

For $[Au(\mathbf{L^1})_2Cl_2]Cl$ **2**, there are two reduction peaks (A and B) and three oxidation peaks (C, D and E). The first reduction peak A (*ca*. -0.11 V) is tentatively assigned[5] to the reduction of Au^{III} to Au^{I}. Peak B is presumably related to the reduction of Au^{I} to Au^{0} and the reverse process emerges at peak C. This type of quasi-reversibility has been observed[5,6] at similar potentials for other Au^{I}-NHC complexes. Peaks D and E are tentatively attributed respectively to the oxidation of chloride (Cl^-/ 0.5 Cl_2) and the oxidative dissolution of deposited Au^0 on the electrode to Au^{I} species. These oxidation processes have been observed[5,7] at similar potentials in cyclovoltammetric studies of other Au^{I}-NHC species. In the cyclic voltammograms of $[Au(\mathbf{L^1})_2](PF_6)_3$ **5**, the processes are observed at similar potentials as seen for $[Au(\mathbf{L^1})_2Cl_2]Cl$ **2**, except there is no peak for oxidation of chloride. The Cl^- and PF_6^- salts of the Au^{III} complexes $\mathbf{L^2}$ and $\mathbf{L^3}$ displayed similar cyclic voltammograms to those seen for $[Au(\mathbf{L^1})_2Cl_2]Cl$ **2** and $[Au(\mathbf{L^1})_2](PF_6)_3$ **5**. We saw no evidence for a wave that could be attributed to an Au^{II} intermediate in cyclic voltammetry studies of any of the Au^{III} complexes.

References

1. M. P. Suh, I. S. Kim, B. Y. Shim, D. Hong and T.-S. Yoon, *Inorg. Chem.*, 1996, **35**, 3595-3598.
2. G. Nardin, L. Randaccio, G. Annibale, G. Natile and B. Pitteri, *J. Chem. Soc., Dalton Trans.*, 1980, 220-223.
3. R. Elder and J. Watkins, *Inorg. Chem.*, 1986, **25**, 223-226.
4. V. Duckworth and N. Stephenson, *Inorg. Chem.*, 1969, **8**, 1661-1664.
5. H. V. Huynh, S. Guo and W. Wu, *Organometallics*, 2013, **32**, 4591-4600.
6. C. Tubaro, M. Baron, M. Costante, M. Basato, A. Biffis, A. Gennaro, A. A. Isse, C. Graiff and G. Accorsi, *Dalton Trans.*, 2013, **42**, 10952-10963.
7. B. Ballarin, L. Busetto, M. C. Cassani and C. Femoni, *Inorg. Chim. Acta*, 2010, **363**, 2055-2064.